9964 *Macromolecules* **2010**, *43*, 9964–9971
DOI: 10.1021/ma1022764

Macromolecules
ARTICLE

Thermoresponsive Copolymer Hydrogels on the Basis of *N*-Isopropylacrylamide and a Non-Ionic Surfactant Monomer: Swelling Behavior, Transparency and Rheological Properties

Tatjana Friedrich and Bernd Tieke*

University of Cologne, Department of Chemistry, Luxemburger Strasse 116, D-50939 Cologne, Germany

Florian J. Stadler[†] and Christian Bailly

Université catholique de Louvain, Institut de la Matière condensée et des Nanosciences, Croix du Sud, 1, B-1348 Louvain-la-Neuve, Belgium. [†]Present address: Chonbuk National University, School of Semiconductor and Chemical Engineering, 664-14, 1-ga Deokjin-dong, Deokjin-gu, Jeonju, Jeonbuk, 561-756, Republic of Korea

Thomas Eckert and Walter Richtering

RWTH Aachen University, Institute of Physical Chemistry, Landoltweg 2, D-52056 Aachen, Germany

Received July 15, 2010; Revised Manuscript Received November 2, 2010

ABSTRACT: Copolymer hydrogels were prepared upon γ-ray-induced polymerization of aqueous micellar solutions containing *N*-isopropylacrylamide (NiPAAm) and the surfactant monomer (surfmer) ω-methoxy poly(ethylene oxide)$_{40}$undecyl-α-methacrylate (PEO-R-MA-40). Stable, transparent, and thermosensitive hydrogels were obtained in a one-step process. Dose versus conversion measurements showed a complete conversion of comonomer solutions to hydrogels. The size of the surfmer micelles prior and subsequent to polymerization was studied using SAXS measurements. Presence of NiPAAm in the aqueous phase did not influence the size of the PEO-R-MA-40 micelles. During the polymerization process the particle diameter decreased from 7.0 to 5.6 nm probably due to cross-linking in the shell of the micelles. The thermosensitive behavior of the copolymer gels was investigated. The lower critical solution temperature (LCST) of the surfmer-containing gels was higher than for pure poly-NiPAAm (P-NiPAAm) gels, the increase being a direct function of the surfmer concentration. For hydrogels containing small amounts of surfmer, the shrinking at temperatures above the LCST was increased, and the swelling behavior at temperatures below the LCST was slightly increased. The mechanical stability of the copolymer hydrogels was studied using elongational deformation measurements. Presence of surfmer increased the mechanical stability of the hydrogels, the true stress at break being clearly higher for the copolymer gels compared with pure P-NiPAAm gels. A hydrogel containing only 1% (w/w) of surfmer can be elongated up to a true stress being nearly twice as large as for the pure P-NiPAAm gel. This can be explained by the presence of copolymerized micellar aggregates acting as new, stable cross-linking units. A structure model correlating the mechanical properties with a possible network structure is presented.

1. Introduction

Thermoresponsive hydrogels based on *N*-isopropylacrylamide (NiPAAm) have attracted much attention in soft matter research in recent years. If heated above 32 °C, the lower critical solution temperature (LCST) of the hydrogel, they show a reversible phase transition involving clouding of the hydrogel network and expulsion of incorporated water.[1,2] This property renders the poly-NiPAAm (P-NiPAAm) hydrogels attractive for applications in fields of sensors, actuators, switches and drug delivery systems.[3−13] Pure P-NiPAAm gels are restricted in their applications due to a poor shrinking behavior[14,15] and weak mechanical stability.[16] One way to improve the shrinking properties is to incorporate surfactants in the hydrogels. Probably the earliest study was reported by Yu and Grainger,[17] who prepared amphiphilic thermosensitive terpolymer hydrogels by micellar polymerization of NiPAAm, long chain *N*-alkylacrylamides and sodium acrylate in presence of surfactants such as sodium dodecyl sulfate. Within the hydrogels the *N*-alkylacrylamides were stabilized by sodium dodecyl sulfate, the surfactant being partially incorporated in the network. In subsequent studies, the incorporation of polymerizable surfactants (surfactant monomers, surfmers) in P-NiPAAm hydrogels was reported. Surfactant homopolymers were first prepared followed by polymerization of NiPAAm in the presence of the polymerized surfmer.[18,19] Pendant micellar structure within hydrogels could be obtained upon copolymerization of NiPAAm with a previously synthesized linear NiPAAm-surfmer macromonomer.[20] NiPAAm hydrogels with grafted ionic surfactants were found to show a rapid shrinking due to micelle formation of the copolymerized surfactants above the lower critical solution temperature of the hydrogel.[21,22] Recently, we succeeded in the preparation of NiPAAm−surfmer copolymer hydrogels in a one-step process upon γ-ray induced polymerization of micellar monomer solutions of NiPAAm and a cationic surfmer.[14,23,24] The hydrogels showed an improved, fully reversible swelling behavior. Furthermore, the copolymerized micelles acted as additional cross-linking sites, thereby increasing the mechanical stability of the hydrogels.[25]

---

*Author to whom correspondence should be addressed. E-mail: tieke@uni-koeln.de. Telephone: +49 221 470 2440. Fax: +49 221 470 7300.

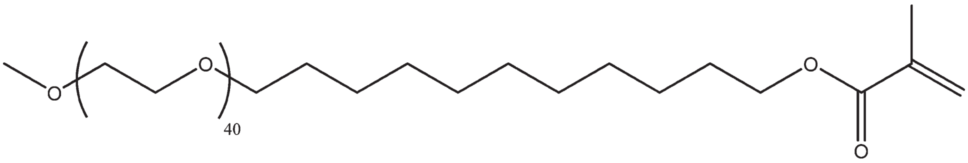

Figure 1. Molecular structure of nonionic surfmer PEO-R-MA-40.

The aim of the present study is to characterize the influence of the nonionic surfmer PEO-R-MA-40 (Figure 1) on the properties of P-NiPAAm hydrogels. We assume that the chemical and physical properties of the PEO-R-MA-40/NiPAAm hydrogels differ from copolymer gels prepared with ionic surfmers. The swelling/shrinking behavior of gels containing nonionic surfmer should be independent from the presence of salt in the aqueous phase because, in contrast to the charged gels based on P-NiPAAm and a cationic surfmer,[14] no osmotic effect should occur. The LCST of the PEO-R-MA-40-containing gels should be more variable than for the gels containing ionic surfmers, because any effect of headgroup dissociation is missing. Furthermore, we were interested in the interactions of nonionic surfmers with NiPAAm molecules, which strongly influence the structure of the network obtained after copolymerization, and the mechanical properties of the copolymer gels, too.

In the following, the thermoresponsive behavior such as changes in volume and transparency, and the mechanical properties of the copolymer hydrogels are investigated, and the effect of the surfmer concentration is studied. The results from the mechanical characterization are explained by a structure model that takes into account the phase behavior and the SAXS characterization of the gels.

2. Experimental Section

2.1. Materials. ω-Methoxy poly(ethylene oxide)$_{40}$ undecyl-α-methacrylate (PEO-R-MA-40) (Figure 1) was prepared in a four step process according to the literature.[26] At first 11-bromoundecanol (Acros) was reacted with 3,4-dihydro-2H-pyran (Acros) to protect the hydroxyl group followed by reaction with poly(ethylene glycol) methyl ether (Sigma-Aldrich). After hydrolysis of the protecting group the hydroxyl group was retrieved and subsequently reacted with methacryloyl chloride (Fluka). After recrystallization from chloroform and ether 35.1 g of a white powder were obtained (yield: 42.4%). The purity of the surfmer was confirmed by elemental analysis, ^{1}H NMR and FT-IR spectroscopy. The FT-IR spectrum (see Supporting Information) shows the C−H stretching mode at 2870 cm^{-1}, C−O−C bending modes at 1109 cm^{-1}, C═O stretching at 1718 cm^{-1} and C═C stretching at 1637 cm^{-1}. The 1H-NMR spectrum and the peak assignments are shown in the Supporting Information. From the ^{1}H NMR spectrum the average number of C═C units per monomer was calculated upon evaluation of the integral ratios of C═C−H (δ = 6.08 and 5.55) and (CH$_2$)$_7$ (δ = 1.26) signals. A ratio of 1: 7 was found indicating the end-group functionality to be unity. Elemental analysis of $C_{96}H_{190}O_4$: calcd. C 56.73, H 9.42; found C 56.32, H 9.40.

N-Isopropylacrylamide (Acros) was recrystallized from toluene and *n*-hexane (volume ratio: 1: 2). Milli-Q-water was used for all experiments.

Preparation of Hydrogels. Monomer solutions containing 10% (w/w) NiPAAm (0.885 mmol/g) and 1 to 10% (w/w) PEO-R-MA-40 (0.005−0.049 mmol/g) in degassed Milli-Q-water, the molar ratio of NiPAAm to surfmer being between 177:1 and 18:1, were homogenized using a Vortex mixer and aged for 24 h. Subsequently, polymerization was carried out in screw-capped glass tubes (4.5 × 1.4 cm or 7 × 1.8 cm), quartz cuvettes (5 × 1 x 1 cm) or glass capillaries (8 × 0.15 cm) using ^{60}Co-γ-radiation. The samples were placed in the middle of eight circularly arranged ^{60}Co-sources of equal dose rate. The total dose rate was 128.3 Gy/h, and the temperature was 20 °C. For polymerization in quartz cuvettes and small glass tubes 2 g of monomer solution were used, 10 g for the bigger glass tubes and 0.4 g for the glass capillaries. To achieve a complete conversion, each sample was exposed to a γ-ray dose of 80 kGy. For a gel consisting of NiPAAm and PEO-R-MA-40 in 18:1 molar ratio (containing 10% (w/w) NiPAAm and 10% (w/w) surfmer) an elemental analysis was conducted after drying: Anal. Calcd for $1 \times C_{96}H_{190}O_{43} + 18 \times C_6H_{11}ON$: C, 60.22; H, 9.61; N, 6.20. Found: C, 60.13; H, 9.63; N, 6.28.

2.2. Methods. The critical micelle concentration (*cmc*) was determined from static surface tension measurements of aqueous PEO-R-MA-40 solutions at 20 °C using the Du Noüy ring method, and the Krüss digital tensiometer K 10 T. The data points were corrected after Zuidema and Walters,[27] and the corrected surface tension γ was plotted against the surfactant concentration c. Subsequently, the *cmc* was determined from the intersection of the two lines fitted through the data points.

The surface excess concentration Γ was calculated using the Gibbs equation for nonionic surfactants

$$\Gamma = -\frac{1}{2.3RT}\left(\frac{\mathrm{d}\gamma}{\mathrm{d}(\log c)}\right)_T \tag{1}$$

where R is the gas constant and T is the temperature. From Γ, the surface area a_{sur} of a surfactant headgroup at the water/air interface was calculated as

$$a_{sur} = (N_{\mathrm{A}}\Gamma)^{-1} \tag{2}$$

where N_{A} is the Avogadro constant.

Surfmer solutions for surface tension measurements were prepared by successive dilution of a stock solution in Milli-Q-water, the concentration of PEO-R-MA-40 being 1 mmol/L.

The single phase region of micellar PEO-R-MA-40-NiPAAm-water solutions was determined visually from their transparency at 20 °C. The composition was changed by adding small amounts of NiPAAm to the water-surfmer mixture. All samples were thoroughly homogenized using a Vortex mixer and thermostated in a water bath.

Small angle X-ray scattering (SAXS) measurements were carried out at room temperature on a Rigaku S-Max3000 system with a MicroMax −002+ microfocus X-ray generator. Cu Kα radiation (λ = 0.154 nm) was used. Scattering intensities were measured over a scattering vector (q) range from 0.006 to 0.18 Å^{-1} using a sample-to-detector distance of 2250 mm. The scattered intensity was corrected by subtracting the solvent (water) scattering. Samples were measured in glass capillaries (Hilgenberg) of 1.5 mm path length sealed with two-component epoxy resin adhesive.

Scattering data were analyzed by means of classic Guinier approximation assuming a system of monodisperse spherical aggregates using eqs 3 and 4:

$$I(q) = I(0)\exp(-q^2R_G{}^2/3) \tag{3}$$

$$R_m = R_G\sqrt{\frac{5}{3}} \tag{4}$$

where $I(q)$ is the scattering intensity and $I(0)$ the scattering intensity extrapolated to $q = 0$. R_m is the radius of the micelles and R_G the radius of gyration. The radius of gyration was determined from the initial slope of ln $I(q)$ plotted against q^2.

FT-IR spectra were measured using a Perkin-Elmer spectrum 1000 spectrometer. Samples were dried in vacuum at 30 °C and pestled with the 4-fold amount of potassium bromide. The mixture was subsequently pressed in a pellet using a hydraulic press (Perkin-Elmer).

^{1}H NMR spectra were recorded on a Bruker DPX 300 instrument operating at 300 MHz.

Elemental analyses were obtained on a Perkin-Elmer 2400 elemental analyzer.

Dose vs conversion curves of the comonomer solutions were determined gravimetrically. For polymerization 2 g of aqueous solutions containing 10%(w/w) NiPAAm and 1 or 10% (w/w) PEO-R-MA-40 were filled into screw-capped glass-tubes, and exposed to different γ radiation doses at 20 °C. After irradiation, hydroquinone was added to each sample in order to inhibit further polymerization. This process was followed by two shrinking/reswelling cycles in Milli-Q-water at 20 and 60 °C for 2 h to leach out residual monomers. Subsequently the samples were dried in vacuum at 30 °C.

UV/vis measurements were carried out using a Perkin-Elmer Lambda 14 UV/vis spectrometer equipped with a thermostated sample holder. The lower critical solution temperature (LCST) was determined by measuring the gel transmission at 500 nm as a function of temperature. For the measurements, hydrogel samples were used, which were previously prepared in quartz cuvettes (5 × 1 × 1 cm).

Studies of the swelling/deswelling behavior were carried out using hydrogel samples with a total weight of 1.5 g after polymerization. The hydrogels were prepared from aqueous micellar solutions containing 10% (w/w) NiPAAm and 0 to 10% (w/w) PEO-R-MA-40 in quartz cuvettes of 5 × 1 × 1 cm in size. After irradiation, the hydrogels were taken from the cuvette and immersed in 200 mL thermostated Milli-Q-water or physiological salt solution (0.9% (w/w) NaCl) for different time periods. The water uptake (or release) was determined gravimetrically by weighing the hydrogel prior and subsequent to the water treatment. The degree of swelling S was calculated as

$$S = \frac{W_t - W_0}{W_0} \tag{5}$$

where W_t and W_0 are the weights of the sample after and prior to swelling in water. S was determined as a function of time at constant temperature, the temperature being in the range between 20 and 60 °C.

Samples for mechanical characterization were prepared upon cutting half-frozen hydrogels into slices using razor blades. For the elongational measurements, samples of about 20 mm in length with a cross section around 2 × 3 mm^2 were used.

For the determination of the mechanical limit, elongational deformation experiments were performed at constant rate at room temperature. The elongational deformation measurements were conducted using the ARES-EVF. Elongational rates $\dot{\varepsilon}$ of 10, 1, 0.1, and 0.01 s^{-1} were applied. Details of the method for the mechanical characterization are given in the literature.[25] The molecular weight between two cross-linking units can be calculated as

$$M_c = \frac{3 \cdot N_A \rho k T}{E} \tag{6}$$

where E is the plateau modulus in elongation determined as the slope of the true (or Hencky) stress−strain curves in the linear region, N_A is the Avogadro constant, ρ is the density of the gel, T is the temperature, and k is the Boltzmann constant.

3. Results and Discussions

Surface Tension Measurements. Since we wanted to copolymerize NiPAAm and PEO-R-MA-40 in its micellar form, it was necessary to determine the critical micelle concentration (*cmc*) of the surfmer. Therefore, the interfacial properties of the surfactant monomer were studied. Surface tension measurements were carried out using the ring detachment method at 20 °C. The *cmc* at 25 °C has already been reported,[26] but since the polymerization was carried out at 20 °C and the surfmer headgroup increasingly became hydrated, if the temperature was lowered, we determined the *cmc* at 20 °C. In Figure 2, the plot of the surface tension versus the molar surfmer concentration is shown. From this plot a *cmc* of 3.4 × 10^{-4} mol/L could be determined, which is nearly five times larger than the *cmc* found at 25 °C (6.6 × 10^{-5} mol/L).[26] Our measurement shows that PEO-R-MA-40 forms micellar structures above a concentration of 0.07% (w/w) at 20 °C. This value is far below the surfmer content in the monomer solutions used for hydrogel preparation.

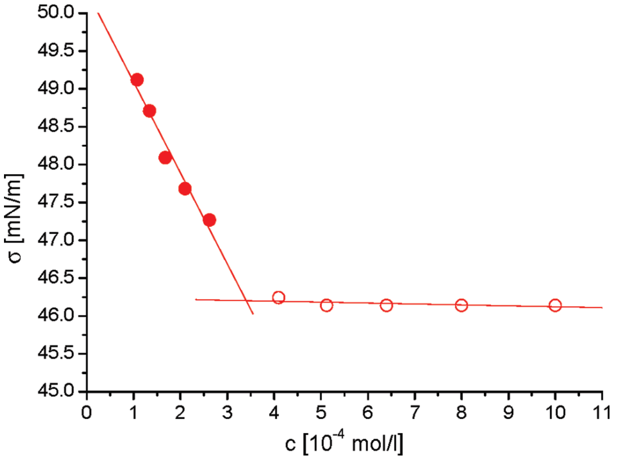

Figure 2. Surface tension vs concentration of nonionic surfmer PEO-R-MA-40 in aqueous solution (T = 20 °C). The symbols represent the measured data points below (closed symbols) and above (open symbols) the *cmc*, the solid lines are obtained by fitting the data points of surface tension in the two regions.

Using eq 2 an area of the surfmer headgroup at the air/water interface of 1,75 nm^2 was calculated. This value was used to calculate the critical packing parameter (*cpp*) of the surfmer using eq 7:[28,29]

$$cpp = \frac{\nu}{a_{sur} l_c} \tag{7}$$

where ν is the volume of a linear alkyl chain of n carbon atoms and l_c its maximum length defined by eqs 8 and 9, respectively:[30]

$$\nu = 0.0274 + 0.0269n \tag{8}$$

and

$$l_c = 0.15 + 0.1265n \tag{9}$$

A *cpp*-value of 0.12 was obtained for PEO-R-MA-40 (for n being 15). Since *cpp*-values of surfactants forming spherical aggregates are known to be up to 0.33, we assume that the PEO-R-MA-40 micelles exhibit a spherical shape although a direct proof of the aggregate structure is still missing.

Phase Behavior of the PEO-R-MA-40-NiPAAm−Water System. In order to prepare clear, transparent hydrogels, it was necessary to start from clear aqueous solutions of the monomeric compounds. Therefore, the phase behavior of the ternary NiPAAm/surfmer/water mixture was investigated and the clear-turbid phase boundaries were determined (Figure 3). If only NiPAAm and no surfmer was present in the aqueous phase, a clear solution formed up to a NiPAAm

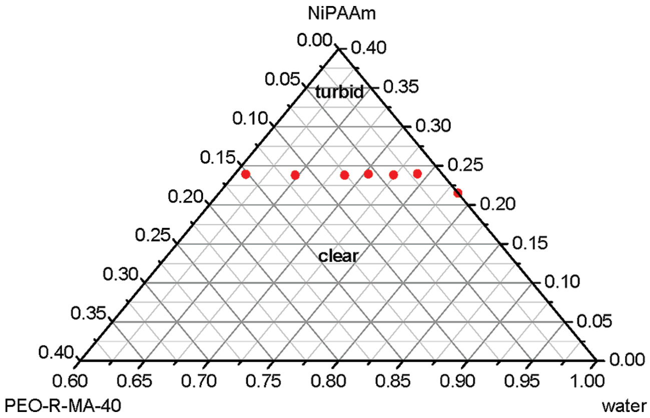

Figure 3. Partial phase diagram of the system PEO-R-MA-40/NiPAAm/water indicating the clear/turbid boundary of the micellar solutions (T = 20 °C).

content of 22% (w/w). Presence of surfmer increased the NiPAAm solubility to 24% (w/w), the solubility being independent of the surfmer concentration in the concentration range investigated. Since the solubility of NiPAAm in the aqueous surfmer solution is almost independent of its concentration, it can be inferred that PEO-R-MA-40 does not interact with NiPAAm. The higher NiPAAm solubility has its origin in the lower surface tension of the aqueous surfmer solution compared with pure water. In principle, the surface tension is only affected by the molecularly dissolved portion of the surfmer molecules. Since this portion is constant above the *cmc*, the solubility of NiPAAm also remains constant at surfmer concentrations above the *cmc*.

Polymerization. Since NiPAAm and PEO-R-MA-40 do not show strong interactions in the monomer solution we assume that the copolymerization proceeds as follows. The methacrylate groups of the surfmer mainly polymerize in the core of the micelles. In the shell of the micelles radicals are formed upon reaction of the ethylene oxide units with hydroxyl radicals resulting from the γ irradiation of the aqueous phase (eq 10 and 11).[31−33]

$$H_2O \xrightarrow{\gamma\text{-ray}} {}^{\bullet}OH, e^-_{aq}, H^{\bullet}, H_2O_2, H_2, H^+ \qquad (10)$$

$$-CH_2-CH_2-O- + {}^{\bullet}OH \rightarrow -CH_2-\dot{C}H-O- + H_2O \qquad (11)$$

The radicals may initiate grafting of NiPAAm or cross-linking of adjacent poly(ethylene oxide) chains.

The process of polymerization was studied by measuring the dose versus conversion behavior for monomer solutions containing 10% NiPAAm and 1 or 10% PEO-R-MA-40. Details are given in the Experimental Section. In Figure 4, the conversion is plotted as a function of radiation dose (dose rate: 128.3 Gy/h). For comparison, the dose vs conversion curve of the homopolymerization of NiPAAm[14] is also shown. It can be seen that the copolymerization proceeds very rapidly. A dose of about 20 kGy is sufficient to obtain a complete conversion of both comonomer solutions into hydrogels. Compared with the polymerization of pure NiPAAm in aqueous solution, the polymerization is slower and longer induction periods occur. Furthermore, the dose, which is necessary to obtain 100% conversion, increases with increasing surfmer concentration. For preparation of hydrogels, we exposed the comonomer solutions to high radiation doses of 80 kGy to ensure a total conversion to hydrogel.

The composition of the hydrogels was studied using IR spectroscopy (see Supporting Information) and elemental analysis (see Experimental Section). In the copolymer IR-spectra the characteristic features of the two components are obvious. The C=O stretching modes at 1652 and 1718 cm^{-1} as well as the N−H and the C−O−C absorption modes at 3430 and 1109 cm^{-1} indicate the presence of P-NiPAAm and P-PEO-R-MA-40 portions in the gel.

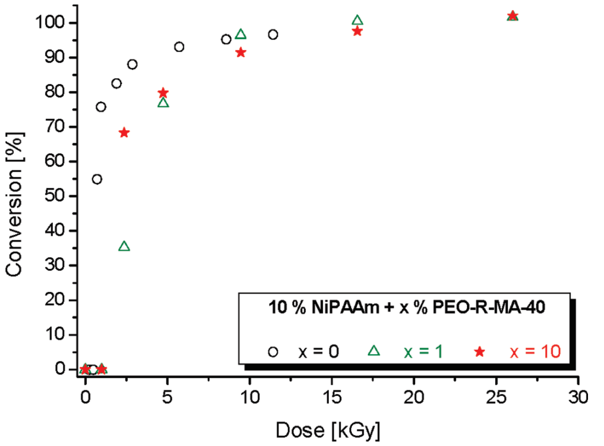

Figure 4. Dose vs conversion curves of pure NiPAAm and NiPAAm-PEO-R-MA-40 comonomers in aqueous solution (dose rate: 128.3 Gy/h, T = 20 °C).

SAXS Measurements. SAXS-measurements were carried out to determine the size of the PEO-R-MA-40 micelles in the monomer solutions and the polymer particles formed in the hydrogel. As known from the literature, the difference in electron density between hydrophobically modified poly(ethylene oxide) copolymers and water leads to a scattering contrast which allows to determine the size of micelles in aqueous solution.[34,35]

First aqueous solutions containing 5% (w/w) surfmer, and 5% (w/w) surfmer and 10% (w/w) NiPAAm were investigated to determine the influence of NiPAAm on the size of the micelles. Subsequently a hydrogel prepared from an aqueous solution containing 5% (w/w) PEO-R-MA-40 and 10% (w/w) NiPAAm was measured. In Figure 5 a, the SAXS curves of the systems are shown. The corresponding Guinier plots are shown in Figure 5 b. The sizes of the micelles and polymer particles were calculated from the slope of the Guinier plots using eqs 3 and 4.

For the monomer solutions similar radii of 3.5 ± 0.1 and 3.6 ± 0.1 nm were found for the systems with and without NiPAAm, respectively. This result is consistent with the absence of interaction between NiPAAm and PEO-R-MA-40 already observed in the study on the phase behavior (Figure 3). If the comonomer solution is irradiated, the Guinier plot shows a lower slope indicating a smaller particle size. For the polymer particles in the hydrogel a radius of 2.8 ± 0.1 nm was calculated. The smaller size of the copolymerized particles can be explained by a grafting of NiPAAm to radicals formed in the poly(ethylene oxide) chains in the shell. Additional cross-linking of poly(ethylene oxide) chains may also occur. Both effects cause a denser packing in the headgroup region of the surfmers and the shell becomes smaller. Some surfmer chains may also be pulled out of the micelles during the copolymerization, leading to a decrease in the aggregation number of the micelles and to a smaller particle size.

Lower Critical Solution Temperature and Gel Transparency. The thermoresponsive behavior of copolymer hydrogels was studied by measuring the change in light transmittance at 500 nm as a function of temperature (Figure 6 a). The influence of the surfmer concentration on the LCST was investigated and compared with the pure P-NiPAAm hydrogel, which has

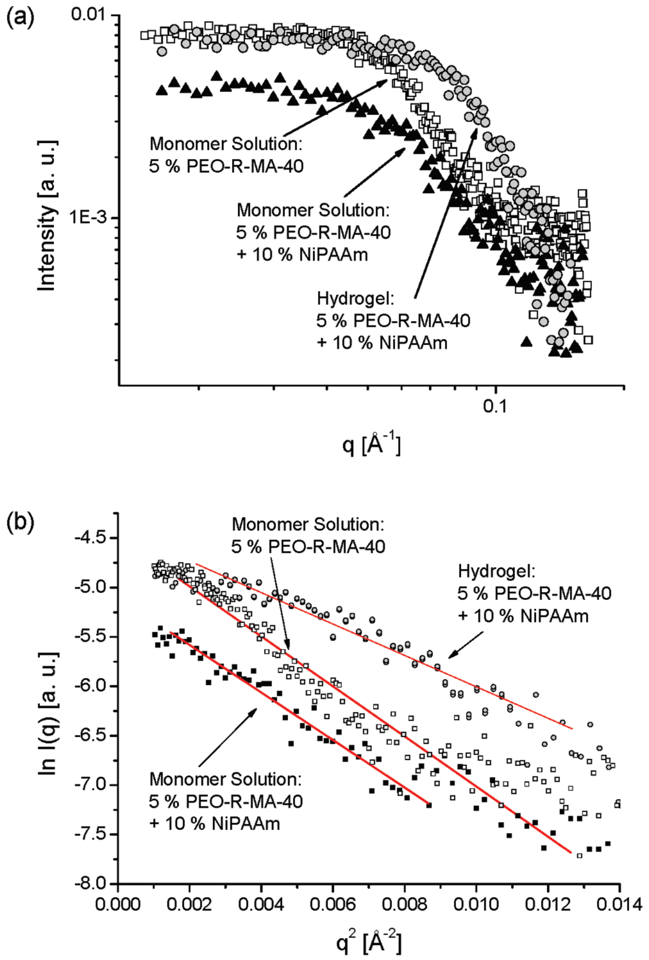

Figure 5. SAXS curves of PEO-R-MA-40 micelles in aqueous monomer solution with and without addition of NiPAAm and copolymerized surfmer micelles in the hydrogel (a) and corresponding Guinier plots (b). Each sample contains 5% (w/w) surfmer.

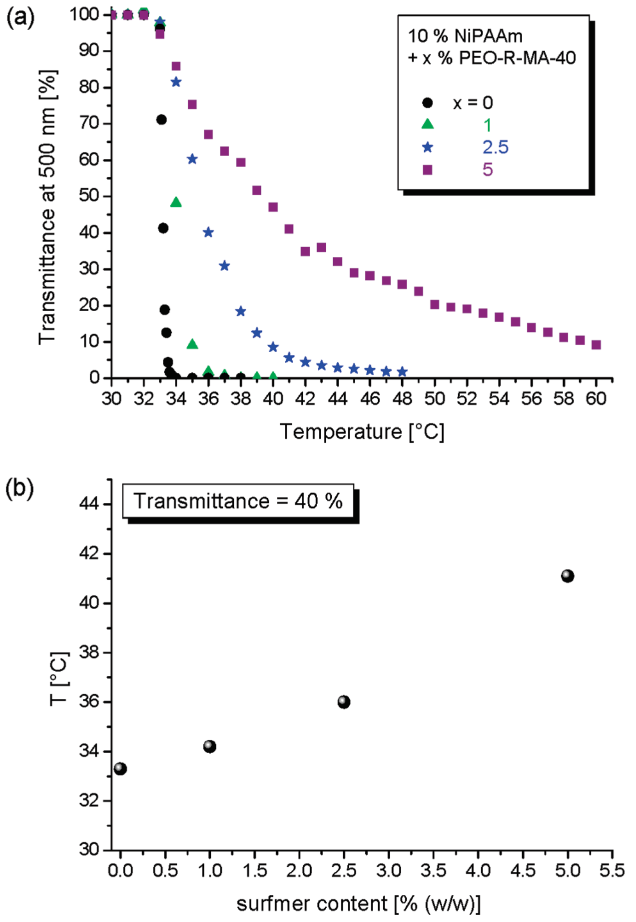

Figure 6. Transparency of various NiPAAm/PEO-R-MA-40-hydrogels and pure P-NiPAAm gel as a function of temperature ($\lambda = 500$ nm).

already been reported.[14] In Figure 6 b the temperature at which a transmittance of 40% is reached is plotted versus the surfmer concentration, for comparison. The P-NiPAAm hydrogel shows a very sharp transition from high to low transparency, if the LCST of the gel of 33.2 °C is reached (Figure 6 a). Upon addition of PEO-R-MA-40, the LCST increases. The more surfmer is added, the higher the LCST becomes. Since the surfmer is very hydrophilic, its presence renders the gel more hydrophilic, which explains the increase of the LCST. As also shown in Figure 6 a, the phase transition range broadens with increasing surfmer content. Clouding of the hydrogel network always starts at the same temperature, both for the pure P-NiPAAm gel and for all surfmer containing gels. The transmission curves reflect the competition between the hydrophobic interaction in the P-NiPAAm portion and the hydrophilic effect of the PEO-containing portions on the phase transition of P-NiPAAm.[36] Introducing more surfmer leads to shorter P-NiPAAm blocks connecting the micelles. This favors the increase of the LCST and the broadening of the transition.

Swelling Behavior. The swelling behavior was studied for hydrogels containing different surfmer concentration. For this purpose, gels were immersed in pure water for different time periods. The weight increase or decrease of the samples was determined gravimetrically and the swelling ratio *S* was calculated using eq 5. In Figure 7, swelling ratios at 20 and 50 °C are plotted versus the immersion time. For the temperature below the LCST, it can be seen that the pure P-NiPAAm gel and hydrogels containing up to 5% (w/w) PEO-R-MA-40 show a similar time-dependence of *S*. With increasing surfmer concentration, the *S*-value slightly increases, because the larger amounts of copolymerized PEO-R-MA-40 render the hydrogels more hydrophilic. Above the LCST, the P-NiPAAm gel only exhibits a moderate shrinking of −0.37 g/g. Shrinking is essentially finished after 1 h as already reported.[14] The reason for the shrinking behavior of the pure gel is the formation of a hydrophobic skin at the surface of the hydrogel, the skin being impermeable to water molecules. In surfmer-containing gels the formation of an impermeable skin is prevented by the presence of hydrophilic copolymerized micelles, which render the gels more permeable to water. As a consequence, the hydrogels containing copolymerized surfmer exhibit a more intense shrinking and the shrinking process takes a longer time. For a hydrogel containing 1% surfmer shrinking is complete after 7 h, whereas for the gels with higher PEO-R-MA-40 concentrations, shrinking is not finished after the investigated time period of 8 h. The highest shrinking after 8 h was found for the hydrogels with the lowest surfmer concentration (−0.76 g/g), and a decrease in shrinking with increasing PEO-R-MA-40 content was observed. The latter can be explained by the increasing hydrophilicity of the system. It partially compensates the thermosensitive behavior of the P-NiPAAm portion of the network. The effect of increasing hydrophilicity can be clearly seen for the swelling of hydrogels at temperatures near to the LCST of the pure P-NiPAAm hydrogel. In Figure 8, swelling ratios at 40 °C are plotted versus the immersion time of hydrogels containing different

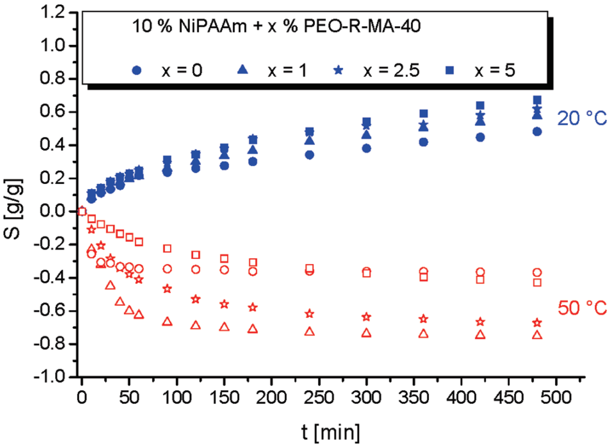

Figure 7. Swelling ratio *S* of pure P-NiPAAm and PEO-R-MA-40/NiPAAm copolymer hydrogels of different composition in water at 20 and 50 °C as a function of time.

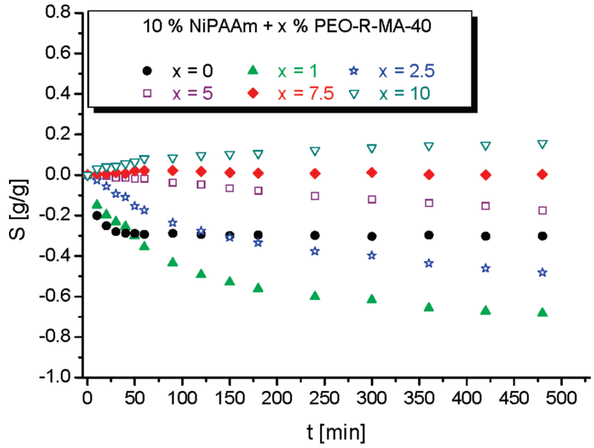

Figure 8. Swelling ratio *S* of a pure NiPAAm hydrogel and PEO-R-MA-40/NiPAAm copolymer hydrogels of different composition in water at 40 °C as a function of time.

amounts of PEO-R-MA-40. Shrinking decreases with increasing surfmer concentration until a concentration of 5% (w/w) is reached. At a concentration of 7.5% (w/w) PEO-R-MA-40, the weight of the hydrogel nearly remains constant and a hydrogel containing 10% (w/w) surfmer shows a moderate swelling.

The influence of salt addition on the swelling behavior of the copolymer gels was also investigated. Therefore, the hydrogels were immersed in physiological salt solution at 20 °C and the swelling was measured as a function of time (for a plot of S vs time see the Supporting Information). The swelling is only slightly diminished, if salt is present in the aqueous solution. The lower *S*-values can be explained by the induction of an osmotic pressure difference between the gel and the surroundings, which opposes the swelling.

Elongation Measurements. Since we were interested in the effect of copolymerized surfmers on the mechanical stability of NiPAAm hydrogels, the mechanical behavior of surfmer/NiPAAm gels with different surfmer concentration was investigated. In order to obtain information on the limits of mechanical stability, nonlinear elongational measurements were performed. In Figure 9, the true stress is plotted as a function of Hencky-strain for hydrogels containing 10% (w/w) NiPAAm and different amounts of PEO-R-MA-40. It can be seen that the addition of surfmer leads to an increase in stiffness. The E-modulus increases from 14 kPa for the pure P-NiPAAm gel to 37 kPa for a hydrogel containing additional 7.5% (w/w) PEO-R-MA-40. Hencky-strain and true stress at break are increased upon surfmer addition. The influence of surfmer concentration on the limit of mechanical stability is shown in Figure 10. For surfmer concentrations up to 5% (w/w), stress and strain at break, $\sigma_{H,max}$ and $\varepsilon_{H,max}$, respectively, increase with increasing surfmer concentration. A hydrogel containing 5% (w/w) can be elongated up to a true stress of 90 kPa being more than two and a half times larger than for the pure NiPAAm gel. For hydrogels with higher surfmer concentration the true stress at break is lower. A hydrogel containing 7.5% (w/w) breaks at a stress $\sigma_{H,max}$ of 78 kPa. For a concentration range between 1 and 5% (w/w), the Hencky strain at break also increases with increasing surfmer concentration. A hydrogel containing 1% PEO-R-MA-40 can be deformed up to a Hencky-strain $\varepsilon_{H,max}$ of 1.0, a hydrogel containing the 5-fold amount of surfmer breaks at a Hencky strain of 1.2. Further increase of the surfmer concentration leads to hydrogels, which are less ductile, the Hencky strain at break being similar to the one observed for the pure P-NiPAAm gel.

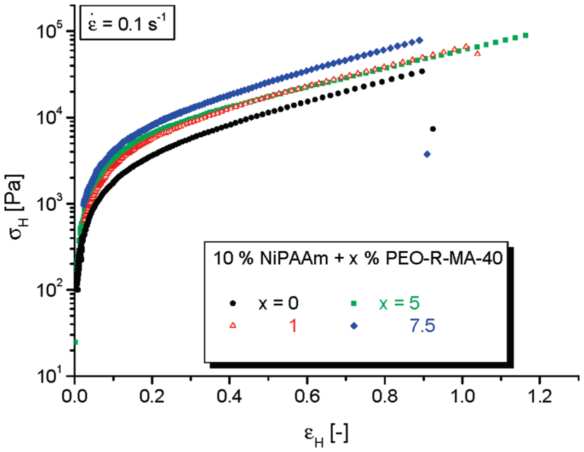

Figure 9. True stress vs Hencky strain for a pure NiPAAm-hydrogel and PEO-R-MA-40/NiPAAm-hydrogels containing 10% (w/w) NiPAAm. Elongation rate: 0.1 s^{-1}.

The molecular weight M_c between two cross-linking sites was calculated using eq 6. In Figure 11, M_c is plotted versus the surfmer concentration of the hydrogels. M_c decreases with increasing surfmer concentration. For the pure NiPAAm gel, the molecular weight between the cross-linking sites is 531 kg/mol. Upon surfmer addition, M_c decreases until the hydrogel containing 7.5% (w/w) PEO-R-MA-40 exhibits $M_c = 201$ kg/mol. Since the molecular weight of chains between two cross-linking sites affects the deformability, the Hencky strain at break is decreased for the highly cross-linked hydrogels containing 7.5% (w/w) PEO-R-MA-40. This can be understood as a balance between the reduction of the stretched chain length and the distance between the cross-linking points. The ratio between these two quantities gives the maximum stretch that a rubber-like material such as the hydrogels can withstand without damage.

To examine the influence of M_c on the true stress at break, the stress−strain behavior of a pure P-NiPAAm hydrogel containing 15% NiPAAm, was investigated. Its M_c value of 212 kg/mol is similar to the surfmer/NiPAAm copolymer gel containing 7.5% PEO-R-MA-40, which means that both gels exhibit a similar cross-linking density. In the following, the mechanical properties of the gel containing 15% (w/w) NiPAAm were compared with the properties of the PEO-R-MA-40-containing hydrogel and a P-NiPAAm hydrogel with lower

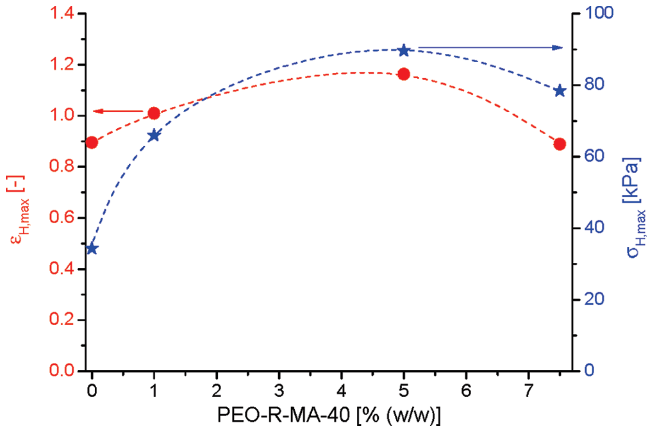

Figure 10. Hencky strain at break and true stress at break as a function of surfmer-content for PEO-R-MA-40/NiPAAm hydrogels containing 10% (w/w) NiPAAm.

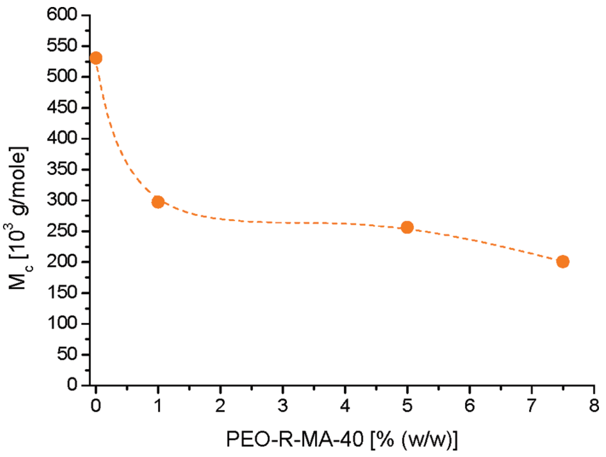

Figure 11. Molecular weight between two cross-linking sites as a function of surfmer-content for hydrogels containing 10% (w/w) NiPAAm.

solid content of 10% (w/w) and a higher cross-linking molar mass M_c of 531 kg/mol (Figure 12). On one hand the higher cross-linking density of the gel with 15% NiPAAm compared with the gel with 10% NiPAAm influences the Hencky-strain at break, which is decreased to 0.72. Because of the enhanced cross-linking density, the gel containing more P-NiPAAm is less ductile. On the other hand, the true stress at break is very similar for both pure P-NiPAAm gels. Therefore, we assume that an increase in cross-linking density due to a higher NiPAAm concentration does not really increase the mechanical stability of the hydrogels. The gel containing 7.5% (w/w) surfmer can be elongated to a $\sigma_{H,max}$ value more than twice as large although the cross-linking density is the same. This indicates that the copolymerized micelles represent stronger cross-linking sites than the radiation-induced cross-linking sites in the P-NiPAAm portion of the network.

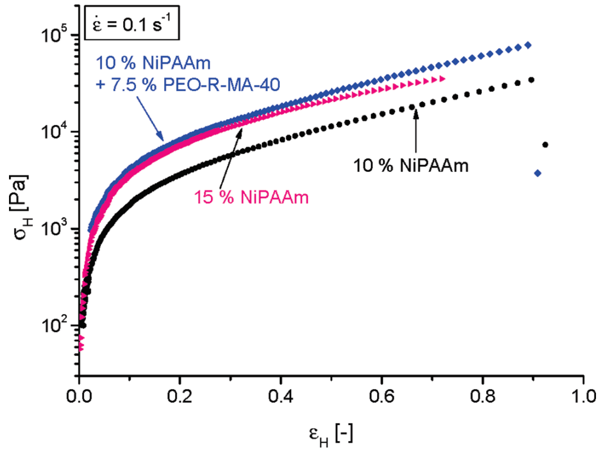

Figure 12. True stress vs Hencky strain for pure NiPAAm-hydrogels containing 10 or 15% NiPAAm and a PEO-R-MA-40/NiPAAm-hydrogel containing 10% (w/w) NiPAAm and 7.5% surfmer. Elongation rate: 0.1 s^{-1}.

Scheme 1. Schematic Illustration of a Pure NiPAAm Network (a) and a NiPAAm/Surfmer Network (b)[a]

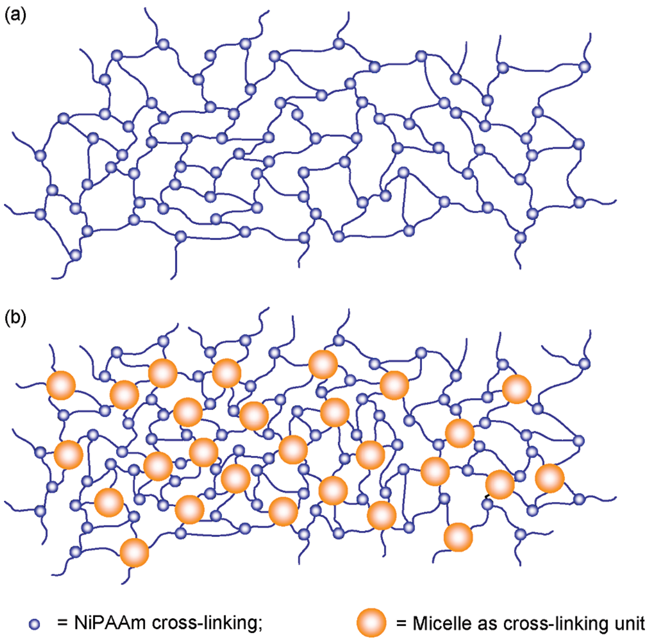

[a] The blue spheres demonstrate NiPAAm cross-linking units, the orange ones are cross-links formed by micelles.

A structure model taking into account the phase behavior of the monomeric solution as well as the results of the SAXS measurements and the mechanical characterization of the hydrogels is shown in Scheme 1. In the monomeric solution, NiPAAm molecules as well as surfmer micelles are present, which do not strongly interact in contrast to NiPAAm and micelles of cationic surfmers. During polymerization the copolymerized micelles form new cross-linking sites in addition to the cross-links formed during NiPAAm polymerization. Consequently, the copolymer hydrogels are more strongly cross-linked than the pure P-NiPAAm gels, resulting in smaller M_c-values. The new junctions are more stable than the P-NiPAAm based ones. Therefore, the copolymer hydrogels can be deformed to a higher true stress.

4. Conclusions

In our contribution, it is demonstrated that P-NiPAAm-based hydrogels containing the nonionic surfmer PEO-R-MA-40 can be prepared in a single step process upon γ-ray induced copolymerization of aqueous micellar solutions. The copolymer hydrogels show an increased mechanical stability. The mechanical properties can be ascribed to the copolymerized micelles acting as additional strong cross-linking sites. Presence of hydrophilic surfmer also prevents the formation of an impermeable skin at the surface of the hydrogels. Therefore, an improved shrinking behavior is obtained at low surfmer concentrations. Upon addition of surfmer, the lower critical solution temperature can be varied over a wide range due to the increasing hydrophilicity of the hydrogel network with increasing PEO-R-MA-40 content.

Different from ionic surfmers, no interaction of NiPAAm and PEO-R-MA-40 is observed and therefore, the size of the PEO-R-MA-40 micelles in aqueous monomer solution is only little effected by the addition of NiPAAm. The network structures of the copolymer hydrogels containing nonionic and ionic surfmer differ strongly. For hydrogels containing nonionic surfmer, the molecular weight between two cross-linking sites decreases with increasing surfmer concentration, whereas for the gels containing ionic surfmers it increases due to an incorporation of NiPAAm in the copolymerized micelles.[25] Therefore, PEO-R-MA-40 hydrogels are much stiffer. Despite of a low scattering contrast SAXS measurements were found to be an effective tool to determine the size of the polymer particles in the hydrogel network. Upon polymerization the particle size decreases due to cross-linking in the shell of the PEO-R-MA-40 micelles. For the ionic surfmers an increased size was found subsequent to polymerization[14] due to further incorporation of NiPAAm in the micelles during the copolymerization process.

Acknowledgment. The DFG is thanked for financial support (Project TI 219/10-1 and 10-2, priority program 1256 “Intelligent Hydrogels”).

Supporting Information Available: Figures showing ^{1}H NMR and IR spectra of PEO-R-MA-40, IR spectra of dried hydrogels, polymerized surfmer and P-NiPAAm, photographic image of a hydrogel, time dependence of swelling ratio at various temperatures, comparative plot of swelling ratio vs time at 20 and 50 °C for hydrogels containing different surfmer concentration, swelling ratio at 20 °C in physiological salt solution. This material is available free of charge via the Internet at http://pubs.acs.org/.

References and Notes

(1) Heskins, M.; Guillet, J. E. *J. Macromol. Sci., Chem.* **1968**, *A2*, 1441–1455.
(2) Hirokawa, Y.; Tanaka, T. *J. Chem. Phys.* **1986**, *81*, 6379–6380.
(3) Nayah, S.; Lyon, L. A. *Angew. Chem.* **2005**, *117*, 7862–7886.
(4) Richter, A.; Paschew, G.; Klatt, S.; Lienig, J.; Arndt, K.-F.; Alder, H.-J. P. *Sensors* **2008**, *8*, 561–581.
(5) Gupta, P.; Vermani, K.; Garg, S. *Drugs Discovery Today* **2002**, *7*, 569–579.
(6) Jeong, B.; Gutowska, A. *Trends Biotechnol.* **2002**, *20*, 305–311.
(7) Dagani, R. *Chem. Eng. News* **1997**, *75*, 26–37.
(8) Thiel, J.; Maurer, G.; Prausnitz, J. M. *Chem. Ing. Techn.* **1995**, *67*, 1567–1583.
(9) Schexnailder, P.; Schmidt, G. *Colloid Polym. Sci.* **2009**, *287*, 1–11.
(10) Kuckling, D. *Colloid Polym. Sci.* **2009**, *287*, 881–891.
(11) Texter, J. *Colloid Polym. Sci.* **2009**, *287*, 313–321.
(12) Liu, R.; Fraylich, M.; Saunders, B. R. *Colloid Polym. Sci.* **2009**, *287*, 627–643.
(13) Musch, J.; Schneider, S.; Lindner, P.; Richtering, W. *J. Phys. Chem. B* **2008**, *112*, 6309–6314.
(14) Friedrich, T.; Tieke, B.; Meyer, M.; Pyckhout-Hintzen, W.; Pipich, V. *J. Phys. Chem. B* **2010**, *114*, 5666–5677.
(15) Yoshida, R.; Uchida, K.; Kaneko, Y.; Sakai, K.; Kikuchi, A.; Sakurai, Y.; Okano, T. *Nature* **1995**, *374*, 240–242.
(16) Gong, J. P.; Katsuyama, Y.; Kurokawa, T.; Osada, Y. *Adv. Mater.* **2003**, *15*, 1155–1158.
(17) Yu, H.; Grainger, W. *Macromolecules* **1994**, *27*, 4554–4560.
(18) Yan, H.; Fujiwara, H.; Sasaki, H.; Tsujii, K. *Angew. Chem., Int. Ed. Engl.* **2005**, *44*, 1951–1954.
(19) Chen, X.; Tsujii, K. *Macromolecules* **2006**, *39*, 8550–8552.
(20) Xu, X.-D.; Zhang, X.-Z.; Yang, J.; Cheng, S.-X.; Zhuo, R.-X.; Huang, Y.-Q. *Langmuir* **2007**, *23*, 4231–4236.
(21) Noguchi, Y.; Okeyoshi, K.; Yoshida, R. *Macromol. Rapid Commun.* **2005**, *26*, 1913–1917.
(22) Okeyoshi, K.; Abe, T.; Noguchi, Y.; Furukawa, H.; Yoshida, R. *Macromol. Rapid Commun.* **2008**, *29*, 897–903.
(23) Friedrich, T.; Tieke, B. *Macromol. Symp.* **2010**, *287*, 16–21.
(24) Friedrich, T.; Tieke, B. *Colloid Polym. Sci.* **2010**, *288*, 1479–1484.
(25) Friedrich, T.; Tieke, B.; Stadler, F. J.; Bailly, C. Submitted for publication.
(26) Liu, J.; Chew, C. H.; Gan, L. M. *J. Macromol. Sci.—Pure Appl. Chem.* **1996**, *33*, 337–352.
(27) Zuidema, H. H.; Waters, G. W. *Ing. Eng. Chem. Anal. Ed.* **1941**, *13*, 312–313.
(28) Chevalier, Y.; Zembf, T. *Rep. Prog. Phys.* **1990**, *53*, 279–371.
(29) Hoffmann, H. *Prog. Colloid Polym. Sci.* **1990**, *83*, 16–28.
(30) Tenfold, C. *The hydrophobic effect*; Wiley-Interscience: New York, 1980.
(31) Matheson, M. S.; Mamou, A.; Silverman, J.; Rabani, J. *J. Phys. Chem.* **1973**, *77*, 2420–2424.
(32) Savas, H.; Güven, O. *Radiat. Phys. Chem.* **2002**, *64*, 35–40.
(33) Ulanski, P.; Zainuddin; Rosiak, J. M. *Radiat. Phys. Chem.* **1995**, *46*, 913–916.
(34) Sommer, C.; Pederson, J. S.; Garamus, V. M. *Langmuir* **2005**, *21*, 2137–2149.
(35) Hickl, P.; Ballauff, M.; Jada, A. *Macromolecules* **1996**, *29*, 4006–4014.
(36) Virtanen, J.; Baron, C.; Tenhu, H. *Macromolecules* **2000**, *33*, 336–341.